Chemical Science

Accepted Manuscript

Volume 7 | Number 1 | January 2016 | Pages 1–812

Chemical Science

www.rsc.org/chemicalscience

ISSN 2041-6539

ROYAL SOCIETY OF CHEMISTRY

EDGE ARTICLE
Francesco Ricci et al
Electronic control of DNA-based nanoswitches and nanodevices

175 YEARS

This is an Accepted Manuscript, which has been through the Royal Society of Chemistry peer review process and has been accepted for publication.

Accepted Manuscripts are published online shortly after acceptance, before technical editing, formatting and proof reading. Using this free service, authors can make their results available to the community, in citable form, before we publish the edited article. We will replace this Accepted Manuscript with the edited and formatted Advance Article as soon as it is available.

You can find more information about Accepted Manuscripts in the author guidelines.

Please note that technical editing may introduce minor changes to the text and/or graphics, which may alter content. The journal's standard Terms & Conditions and the ethical guidelines, outlined in our author and reviewer resource centre, still apply. In no event shall the Royal Society of Chemistry be held responsible for any errors or omissions in this Accepted Manuscript or any consequences arising from the use of any information it contains.

ROYAL SOCIETY OF CHEMISTRY

rsc.li/chemical-science

Journal Name

ARTICLE

High Performance Catalyst of Shape-specific Ruthenium Nanoparticles for Production of Primary Amines by Reductive Amination of Carbonyl Compounds

Debraj Chandra,*[a] Yasunori Inoue,[bc] Masato Sasase,[cd] Masaaki Kitano,[cd] Asim Bhaumik,[e] Keigo Kamata,[b] Hideo Hosono[bcd] and Michikazu Hara*[bcf]

The creation of metal catalysts with highly active surfaces is pivotal to meet the strong economical demand of the chemical industry. Specific flat-shaped pristine fcc ruthenium nanoparticles having high atomically active {111} facets exposed on the flat surfaces have been developed that act as a highly selective and reusable heterogeneous catalyst for the production of various primary amines at exceedingly high reaction rates by the low temperature reductive amination of carbonyl compounds. The high performance of the catalyst is attributed to the large fraction of metallic Ru as active sites with weak electron donation ability that prevail on the surface exposed {111} facets of flat-shaped fcc Ru nanoparticles. This catalyst exhibits the highest turnover frequency (TOF) of ca. 1850 h^{-1} for the model reductive amination of biomass derived furfural to furfurylamine and operates with a reaction rate approximately six times higher than that of an efficient and selective support catalyst of Ru-deposited Nb$_2$O$_5$ (TOF: ca. 310 h^{-1}).

Introduction

Heterogeneous catalysis based on metal nanoparticles (NPs) constitutes a key technology due to the innumerable applications for the production of indispensable chemical resources.[1-5] Metal NPs deposited on substrates with high surface areas, i.e. support catalysts, have commonly been used as metal catalysts;[6-11] however, they have limited catalytic performance due to the existence of most stable atomic structures (atomically smooth, less active) on the surfaces of these conventional spherical NPs, as predicted by surface science.[12-14] The development of structurally controlled metal NPs with catalytically highly active domains (atomically rough) is one of the most crucial issues in the field of heterogeneous catalysis.[15-17] Significant attention has recently been devoted towards the size, shape and electronic properties of ruthenium (Ru)-based metal catalysts,[18-23] which exhibit significant potential for various applications including ammonia synthesis/decomposition,[22, 23] Fischer-Tropsch synthesis,[24, 25] CO oxidation,[20, 21] and CO/CO$_2$ methanation.[19, 26, 27] In these cases, an activity-structure relationship has been evidenced through the combination of experiments and theory. We recently observed that Ru NPs can be self-organized on calcium amide (Ca(NH$_2$)$_2$) to a specific structure comprising anchored flat Ru particles by strong interaction between Ru and N.[22] The Ru/Ca(NH$_2$)$_2$ catalyst exhibited activity for ammonia synthesis that was an order of magnitude higher than that for conventional Ru catalysts.[22] While catalysis over Ru NPs with such specific morphology has not been investigated to date, such morphology is also expected to exhibit high catalytic performance over a broad platform for the synthesis of valuable chemicals/intermediates.

Primary amines are key intermediates in the chemical industry with extensive applications in the manufacture of polymers, pharmaceuticals, dyes and detergents.[28-32] The catalytic reductive amination of carbonyl compounds with ammonia (NH$_3$) and hydrogen (H$_2$) as nitrogen source and reductant, respectively, is the most practical and valuable approach for the synthesis of primary amines.[33-35,36-50] To date, metal catalysts are reported as the prime candidates for the reductive amination of carbonyl compounds with NH$_3$ and H$_2$, mainly based on several support catalysts of Ni,[39, 40] Cu,[41] Pd,[42] Ru,[43-47] Rh,[44, 48] and Pt,[49] which only operate with moderate reaction rates, even under high H$_2$ pressure (≥4 MPa). Moreover, the selective reductive amination of carbonyl

a. World Research Hub Initiative (WRHI), Institute of Innovative Research, Tokyo Institute of Technology, Nagatsuta-cho 4259, Midori-ku, Yokohama 226-8503, Japan. E-mail: chandra.d.aa@m.titech.ac.jp
b. Laboratory for Materials and Stuctures, Institute of Innovative Research, Tokyo Institute of Technology, Nagatsuta-cho 4259, Midori-ku, Yokohama 226-8503, Japan. E-mail: mhara@msl.titech.ac.jp
c. ACCEL, Japan Science and Technology Agency, 4-1-8 Honcho, Kawaguchi, Saitama, 332-0012, Japan.
d. Materials Research Center for Element Strategy, Tokyo Institute of Technology, Nagatsuta-cho 4259, Midori-ku, Yokohama 226-8503, Japan.
e. Department of Materials Science, Indian Association for the Cultivation of Science, 2A & B Raja S. C. Mullick Road, Jadavpur, Kolkata - 700 032, India.
f. Advanced Low Carbon Technology Research and Development Program (ALCA), Japan Science and Technology Agency (JST), 4-1-8 Honcho, Kawaguchi, Saitama 332-0012, Japan.
Electronic Supplementary Information (ESI) available: [experimental detail, one table, XPS spectrum, TEM image, reuse experiment data, computational free energy diagram]. See DOI: 10.1039/x0xx00000x

compounds (except simple aryl and alkyl aldehydes) to primary amines is typically hindered by the formation of secondary and tertiary amines and/or undesired further-hydrogenated products. We are focused on the specific morphology and atomic structure of a metal catalyst to realize high intrinsic activity and selective response for the quantitative production of primary amines at markedly high reaction rates than with conventional support catalysts, which is difficult and challenging goal. Herein, we first report a new specific flat-shaped pristine fcc Ru-NP based catalyst having active-sites with weak electron-donation power, which enables the highly efficient and selective reductive amination of various carbonyl compounds. The Ru-NP catalyst provides higher reaction rates that are approximately six times that of an efficient support catalyst of Ru-deposited Nb_2O_5.[47]

Results and discussion

Characterization of the structure of Ru NPs.

The Ru-NP catalysts were prepared from Ru-deposited $Ca(NH_2)_2$. The $Ru/Ca(NH_2)_2$ catalyst cannot be used under ambient conditions, because of the extreme instability of $Ca(NH_2)_2$. The removal of $Ca(NH_2)_2$ was confirmed by the lack of a detectable X-ray photoelectron spectroscopy (XPS) peak in the Ca 2p region for the as-obtained Ru-NPs (see the Supporting information, Figure S1). High-angle annular dark-field scanning transmission electron microscopy (HAADF-STEM) analysis was conducted to investigate the microstructure of the Ru NPs. Figure 1a shows small and flat Ru patches over a large domain. No conventional round shaped grains of Ru were observed. However, after the removal of $Ca(NH_2)_2$, the Ru particles tended to aggregate. The average Ru particle size in $Ru/Ca(NH_2)_2$ was estimated to be ca. 2 nm with a narrow particle size distribution.[5e] In contrast, larger particles were observed after the removal of $Ca(NH_2)_2$, as shown in Figure 1a. This was also

Fig. 1 (a) HAADF-STEM and (b) high magnification HAADF-STEM images of Ru-NPs prepared from 10 wt% Ru-deposited $Ca(NH_2)_2$. (c) HAADF-STEM and (d) high magnification HAADF-STEM images of 10 wt% $Ru/Ca(NH_2)_2$.

Table 1 Physicochemical properties and catalytic performance of various Ru catalysts

Entry	Catalyst[a]	S_{BET}[b] ($m^2 g^{-1}$)	S_{Ru}[c] ($m^2 g^{-1}$)	D[d] (%)	d[e] (nm)	2a Yield[f] (%)	TOF (h^{-1})
1[g]	Ru-NP (10)	108	46	11	11.6	99	1850
2[g]	Ru-NP (15)	101	44	11	11.9	95	1670
3[g]	Ru-NP (20)	98	49	12	11.0	93	1400
4	Ru-HCP	86	62	17	7.9	39	290
5	Ru/Nb_2O_5	112	88	24	5.5	59	310
6	Ru/SiO_2	260	151	41	3.3	62	190

[a] Ru-NPs recovered from different weight percentages of Ru loaded on $Ca(NH_2)_2$, as shown in parenthesis. [b] Specific surface area (S_{BET}) obtained from N_2 sorption analysis. [c] Ru surface area (S_{Ru}) and [d] Ru dispersion (D) determined with CO chemisorption and the stoichiometry of CO/Ru = 0.6 was assumed[23]. [e] Ru particle sizes estimated from dispersion. [f] Reaction conditions: catalyst (0.2 mg for Ru-NPs; 20 mg for 1 wt% Ru/Nb_2O_5 and Ru/SiO_2), **1a** (0.5 mmol), MeOH (5 mL), NH_3 (8 mmol), and H_2 (2 MPa), 363 K, 2 h. [g] TOF calculated from **2a** yield at 30 min.
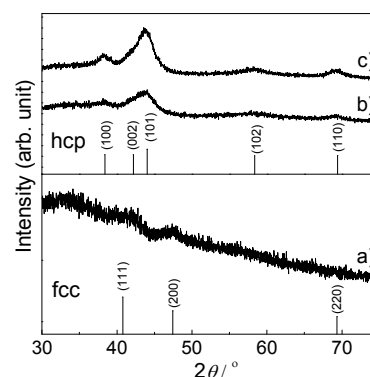

Fig. 2 XRD patterns of Ru-NP samples prepared from (a) 10 wt%, (b) 15 wt% and (c) 20 wt% Ru-deposited Ca(NH2)2. JCPDF card numbers are (hcp) 01-070-0274 and (fcc) 01-088-2333.

confirmed by particle size estimation using CO adsorption on the Ru NP surfaces, as shown in Table 1, where the particle sizes of the Ru-NPs were estimated to exceed 10 nm. The lattice spacing in the Ru NPs (Figure 1b) were observed to be 2.20 Å, which is close to that (d_{111} = 2.21 Å) of the face-centered-cubic (fcc) (111) plane of Ru,[21] and differs from that for the conventional hexagonal-close-packed (hcp) structure (d_{002} = 2.142 Å) of Ru particles.[18, 19] This was also confirmed by

ARTICLE
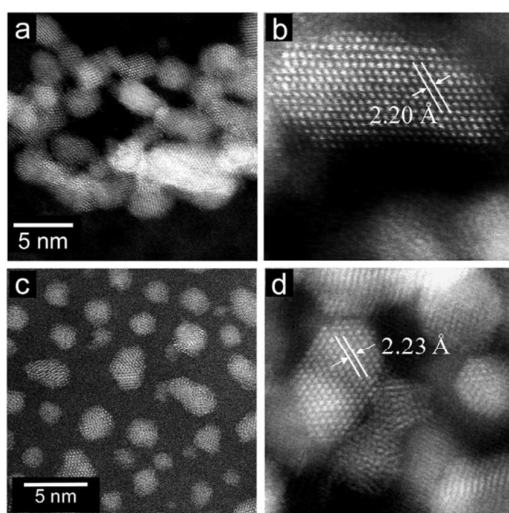
powder X-ray diffraction (XRD) analysis of the Ru NPs (Figure 2a), where broad diffraction peaks due to fcc Ru appear. The morphology of the Ru NPs was not changed significantly compared to that before isolation from Ca(NH$_2$)$_2$ (Figure 1c). There was also no noteworthy difference in the lattice spacing (fcc, d111 = 2.23 Å) of the Ru NPs pre-formed on the Ca(NH$_2$)$_2$ support[22] in Ru/Ca(NH$_2$)$_2$ (Figure 1d), and the NPs structure were successfully preserved in pristine Ru-NP, without stabilization by the interaction between Ru-sites and N after Ca(NH$_2$)$_2$ removal. The possibility of any trace of N element remain bound in the pristine Ru-NPs has been ruled out by the lack of detectable XPS peaks in the N 1s region (Figure S2). Hence, the Ru-sites bound to Ca(NH$_2$)$_2$ in Ru/Ca(NH$_2$)$_2$ are expected to be available in the pristine Ru-NP catalyst. It has been proposed that the presence of abundant {111} facets is essential in fcc Ru nanocrystals for high activity.[21, 24] These flat-shaped fcc Ru NPs are composed of a few atomic layers and could be able to generate a large fraction of open {111} facets exposed on the flat NP surfaces, as suggested by the microstructural analysis. Flat fcc Ru NPs (fcc Ru is a metastable phase compared with hcp Ru[21]) are considered to be stabilized by the strong adhesion between Ru and Ca(NH$_2$)$_2$ during formation, which prevents the growth of large particles (Figure S3). This is also supported by the major growth of gradually larger hcp crystallites (alongside anchored fcc Ru particles) for Ru-NPs prepared from 15 and 20 wt% Ru/Ca(NH$_2$)$_2$, as evident from XRD measurements (Figure 2), presumably due to an increase in the numbers of non-interacted Ru NPs over Ca(NH$_2$)$_2$. HRTEM image (Figure S4) revealed that flat-shaped Ru NPs are intermingled with large particles of hcp Ru grown alongside flat-shaped Ru NPs in Ru-NP (20), Ru-NPs prepared from 20 wt% Ru/Ca(NH$_2$)$_2$.[51] Strong adhesion energy between metal and support has also been reported as a reason for dominant 2D growth (flat-shaped particles) over 3D growth (spherical particles) of other supported metal NPs.[52, 53] The Ru NP sizes obtained from CO chemisorption (Table 1) did not vary significantly for different Ru-NPs and Ru-NPs were larger than those analysed from the HAADF-STEM images, due to aggregation of the NPs after the removal of Ca(NH$_2$)$_2$. XPS analysis (Figure S1) in the Ru 3d region shows two intense narrow peaks at binding energies of 279.9 and 284.0 eV for Ru 3d$_{5/2}$ and 3d$_{3/2}$, respectively. These peaks can be assigned to metallic Ru according to literature,[54-56] which indicates the composition of the NPs is mainly Ru^0. In diffuse reflectance infrared Fourier transform (DRIFT) spectroscopy with CO as a probe molecule, a weak band due to linearly adsorbed CO on partially oxidized Ru [Ru^{n+}-CO; 2069-2086 cm^{-1}] was observed on CO-adsorbed Ru-NPs; a small fraction of Ru surface has been oxidized (Fig. 4, see below).

Catalyst screening for model reductive amination of furfural.

The conversion of biomass-derived[57, 58] furfural (**1a**) to furfurylamine (**2a**) was investigated as a model reaction for reductive amination (Figure 3a). **1a** cannot be completely converted into **2a** over most heterogeneous catalysts (except Ru-deposited Nb$_2$O$_5$, which gives a **2a** yield of 99%[47]), because

the formation of **2a** is thermodynamically unfavourable compared to other byproducts (see Supporting Information). Ru-NPs prepared from Ru-deposited Ca(NH$_2$)$_2$ samples with different loading amounts of Ru (10, 15 and 20 wt%) were tested for initial screening of the catalyst (Table 1 and S1). Ru-NPs prepared from 10 wt% Ru-loaded Ca(NH$_2$)$_2$ provided almost a quantitative yield (99%) of **2a** in 2 h without significant formation of other byproducts (Table S1, entry 1). Ru-NPs prepared from 15 and 20 wt% Ru-loaded Ca(NH$_2$)$_2$ also gave **2a** in high yield (95 and 93%, respectively), although a ring hydrogenated product (tetrahydrofurfurylamine; **5a**) was formed to a significant extent with a total yield of 3-5% along with a small amount of secondary amine (**7a**) through hydrogenation of the dimeric imine **3a** (Table S1, entry 2 and 3). Turnover frequencies (TOFs) for the formation of **2a** were estimated using the dispersion of surface Ru atoms obtained from CO chemisorption (Table 1).[23] The less-selective reductive amination and gradually decreasing TOFs with Ru-NPs obtained from higher Ru loading is perhaps due to the effect of a larger amount of hcp Ru particles with fcc Ru, as suggested by XRD analysis. In fact, a pristine hcp Ru NPs (Ru-HCP, see ESI and Figure S5) catalyst,[24] gives a **2a** yield of only 39% at 2h with much lower TOF (Table 1) and large amount of byproducts (Table S1, entry 4 and 5). In the case of Ru/Nb$_2$O$_5$ and Ru/SiO$_2$, the **2a** yield did not reach 70% at 2 h. Ru-NPs prepared from 10 wt% Ru-loaded Ca(NH$_2$)$_2$ were employed in the following experiments.
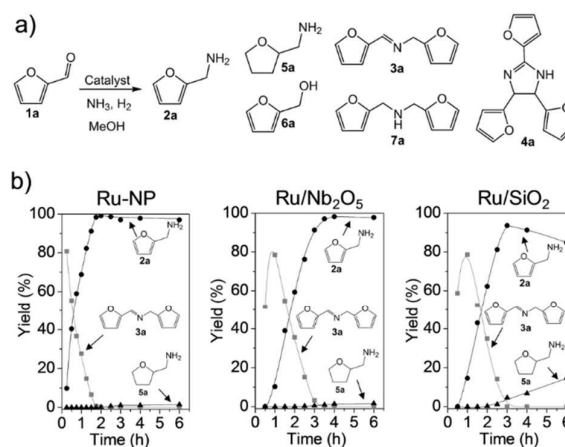

Fig. 3 (a) Catalytic reductive amination of furfural (**1a**) to furfurylamine (**2a**) and related byproducts.[46-48] N-furfurylidenefurfurylamine (**3a**), 2,4,5-tris (2-furyl)imidazoline (**4a**), tetrahydrofurfurylamine (**5a**), furfuryl alcohol (**6a**) and difurfurylamine (**7a**) are the main byproducts. (b) Time courses for the reductive amination of **1a** over Ru-NP, Ru/Nb$_2$O$_5$ and Ru/SiO$_2$ catalysts (Ru: 1 wt% for Ru/Nb$_2$O$_5$ and Ru/SiO$_2$). Reaction conditions: catalyst (0.2 mg for Ru-NP; 20 mg for Ru/Nb$_2$O$_5$ and Ru/SiO$_2$), **1a** (0.5 mmol), MeOH (5 mL), NH$_3$ (8 mmol), and H$_2$ (2 MPa), 363 K.

Performance of Ru-NPs beyond conventional efficient catalysts.

ARTICLE
Journal Name

The time course for the reductive amination of **1a** over Ru-NPs was compared with those for efficient supported metal catalysts of Ru/Nb$_2$O$_5$ and Ru/SiO$_2$ (Figure 3b).[47, 59] In the case of Ru-NPs, **1a** was rapidly converted, and only after approximately 15 min the yield of dimeric imine **3a** reached a maximum. The yield of **2a** gradually increased to 99% at approximately 105 min with a decrease in the yield of **3a**. Hydrogenation products such as **5a**, **6a** and **7a** were not formed

Table 2 Reductive amination of furfural (**1a**) to furfurylamine (**2a**) over various metal catalysts

Entry	Catalyst	Temp. (°C)	pH_2 (MPa)	Time (h)	**2a** Yield (%)	TOF (h^{-1})	Ref.
1	Ru-NP	90	2	2	99	1850	This work
2	Ru-HCP	90	2	5	71	290	This work
3	Ru/Nb$_2$O$_5$	90	2	4	98	310	This work
4	Ru/SiO$_2$	90	2	4	91	190	This work
5	Ru/Nb$_2$O$_5$	90	4	2	99	520	47
6	Ru/TiO$_2$	90	4	4	97	110	47
7	Rh/Al$_2$O$_3$	80	2	2	92	990	48
8	Ru/γ-Al$_2$O$_3$	80	3	2	75	100	45
9	Raney Ni	100	6	3	56	1	60
10	CoReMo	75	9	3	88	-	60
11	Ru/HAP	100	0.3	2	60	6	46

to any substantial extent, even after the catalytic test was conducted for 6 h. Ru/Nb$_2$O$_5$ also gave a **2a** yield of 98% at 4 h without significant progress of other side-reactions, although Ru/Nb$_2$O$_5$ had a much lower rate of **2a** formation than Ru-NPs. This is also supported by the production rate of dimeric imine (**3a**). **3a** was observed even after 3 h over Ru/Nb$_2$O$_5$. On the other hand, it disappeared completely before 2 h in the case of Ru-NPs. Intermediate **3a** produced by the reversible reaction of **1a** and **2a** is expected to be selectively converted into **2a** under the reaction conditions.[47] The Ru/SiO$_2$ catalyst exhibited a similar reaction rate to that of Ru/Nb$_2$O$_5$; however, in a sharp contrast, the subsequent hydrogenation of **2a** into **5a** was observed. It should be noted that an approximate 40% yield of **2a** has been achieved within 30 min over Ru-NPs, which is an approximately three times higher rate than that for the similar yield (at 90 min) of **2a** obtained over either Ru/Nb$_2$O$_5$ or Ru/SiO$_2$. **4a** is formed when the hydrogenation rate of the intermediate furfurylimine (**8a**) to **2a** is not sufficiently high (see Supporting Information).[47] The formation of **4a** was not observed at all over Ru-NPs, whereas the yield of **4a** over Ru/SiO$_2$ exceeded 6%. The TOF for **2a** over Ru-NPs (1850 h^{-1}) was much higher than that over Ru/Nb$_2$O$_5$ (310 h^{-1}) and Ru/SiO$_2$ (190 h^{-1}) irrespective of the lower surface area of Ru in the Ru-NP catalyst (Table 1), which signifies the presence of highly active Ru-sites on the surface of the flat-shaped Ru-NPs.

TOF estimation was also carried out on the basis of active site-poisoning by using 1,10-phenanthroline (see ESI, Figure S6),[61, 62] and the TOFs for Ru-NP (flat-shaped fcc Ru catalyst), Ru/Nb$_2$O$_5$ (efficient supported metal catalyst of hcp Ru) and Ru-HCP (conventional unsupported hcp Ru nanoparticle) were estimated at to 1580 h^{-1}, 370 h^{-1} and 270 h^{-1} respectively, These results are consistent with those estimated by CO adsorption (Table 1). To the best of our knowledge, the Ru-NP catalyst has exhibited the highest TOF among the metal catalysts reported to date for the reductive amination of **1a** to produce **2a** (Table 2).[45, 47, 48] Reuse experiments with the Ru-NP catalyst for the reductive amination of **1a** (Figure S7) showed no noticeable decrease in activity, even after four reuses, which indicates the robustness of the catalyst.

Origin of high performance catalysis over Ru-NPs.

The Ru-NP catalyst is largely superior to the Ru/Nb$_2$O$_5$ in the rate of **2a** formation. However, there is no significant difference in selectivity between the catalysts. A recent report revealed that the yield of **2a** from **1a** is dependent on the electron-donating power of Ru on different supports.[47] Selective reductive amination over Ru/Nb$_2$O$_5$ arises from the weak electron-donating capability of Ru particles on the Nb$_2$O$_5$ surface.[47] Apart from this, only a boost of electron donation to Ru from the support materials was demonstrated.[63-65] However, high performance catalysis over Ru-NPs cannot be explained by such a support-to-metal electronic contribution. To understand the phenomenon, the electronic state of Ru in the Ru-NPs was examined and compared with that in Ru/Nb$_2$O$_5$ and Ru/SiO$_2$ using DRIFT spectroscopy with CO as a probe molecule. As shown in Figure 4, bands were assignable to linearly adsorbed CO on Ru^0 [Ru^0-CO; 2003-2035 cm^{-1}], linearly adsorbed CO on partially oxidized Ru [Ru^{n+}-CO; 2069-2086 cm^{-1}] and tricarbonyl
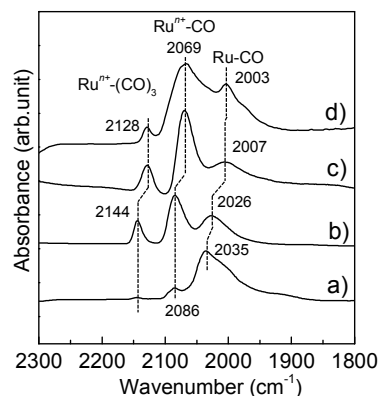

Fig. 4 Difference DRIFT spectra for adsorption of CO onto (a) Ru-NP, (b) Ru/Nb$_2$O$_5$, (c) Ru/SiO$_2$ and (d) Ru-HCP samples at 103 K.

species on partially oxidized Ru [Ru^{n+}-(CO)$_3$; 2128-2144 cm^{-1}].[66, 67] The bands due to CO bonded to Ru/Nb$_2$O$_5$ (2026, 2086, and 2144 cm^{-1}) were blue-shifted more than those of Ru-HCP (2003, 2069, and 2128 cm^{-1}) and Ru/SiO$_2$ (2007, 2069, and

2128 cm^{-1}),[47] due to a decrease of the electron density of Ru by Nb_2O_5 as an acidic (weak electron donating) material.[68] In the case of Ru-NPs, the band for Ru^0-CO (2035 cm^{-1}) was slightly more blue-shifted than that for Ru/Nb_2O_5 (2026 cm^{-1}), although there was no significant difference in the position of the bands for Ru^{n+}-CO (2086 cm^{-1}) and Ru^{n+}-$(CO)_3$ (2144 cm^{-1}), which indicates both the catalysts have comparably weak electron-donating power and would promote selective reductive amination. However, in sharp contrast, the Ru^0-CO band was observed with much higher intensity than Ru^{n+}-CO and Ru^{n+}-$(CO)_3$ for the Ru-NPs, relative to those observed for Ru-HCP, Ru/Nb_2O_5 and Ru/SiO_2. This implies a noticeably large fraction of metallic Ru (rather than oxidized Ru species) as the active sites on the Ru-NPs, which is also in agreement with the XPS analysis. Metallic Ru-species are considered to play an important role for efficient reductive amination. The reductive amination of **1a** did not proceed over a catalyst of RuO_2-deposited Nb_2O_5. However, the high TOF obtained for the Ru-NPs cannot be explained by the large fraction of metallic Ru and the electronic state of Ru-NP. One possible explanation for the catalysis over the Ru-NPs is the atomic structure of the flat-shaped Ru NPs. It has been demonstrated by computational studies that 2D (flat) Ru particles are catalytically more active than hemispherical Ru particles.[23] From computational studies and experiments, it was recently established that the CO dissociation barrier for Fischer-Tropsch synthesis is sufficiently low on the abundant {111} facets of fcc Ru nanocrystals, which results in high mass-specific catalytic activity.[24] CO dissociation barrier on fcc {111} is 1.13 eV, whereas it varies from 0.94-2.37 eV for different facet of hcp Ru.[24] In hcp {0001} facet have lower barrier for CO dissociation, but its sites density is rather low.[19, 24] On the other hand, fcc Ru has abundant {111} facets with slightly higher barrier.[24] Recently, higher activity of fcc Ru compared to hcp Ru was also reported in hydrogenation reaction.[69] This is also clearly demonstrated in the TOF obtained with the Ru-NP catalyst (Table 1). The XRD patterns in Figure 2 reveal that hcp Ru in the obtained Ru-NPs is increased with the amount of Ru-loading on $Ca(NH_2)_2$; excess Ru-loading forms hcp Ru on flat-shaped fcc Ru and decreases the surface exposed {111} facets of fcc Ru. An increase in hcp Ru on Ru-NPs decreases the TOF of Ru-NPs for the reductive amination of furfural, as shown in Table 1. For flat-shaped pristine Ru-NPs, the large fraction of

surface exposed {111} facets (after $Ca(NH_2)_2$ removal Ru-sites become completely free) and electronic state of the Ru-sites possibly affects the adsorption of the substrates and/or the activity of adsorbed hydrogen atoms, which could result in high intrinsic activity for highly efficient reductive amination.

Substrate scope for high performance reductive amination.

Ru-NPs are also effective for the reductive amination of several carbonyl compounds. For example, an important biomass-derived aldehyde, 5-hydroxymethylfurfural (**1b**; a platform chemical for synthesis of several derivatives having potential industrial demand),[57, 58, 70] is efficiently converted into 5-hydroxymethylfurfurylamine (**2b**) in 95% yield (Figure 5). The reaction proceeds with a much higher rate under 4 MPa H_2 to give a 92% yield of **2b** in only 1.5 h, which is approximately 2.5 times higher than that recently reported for an efficient supported metal catalyst (Ru/Nb_2O_5) operated under identical conditions.[47] A broad range of aldehydes and ketones that contain different reduction sensitive functional groups (Table 3), such as alkyl/aryl substituents, halogens and heterocycles, were also successfully tolerated, and the corresponding primary amines were readily produced in noticeably high yields, mostly irrespective of the electronic effects from the functional groups.
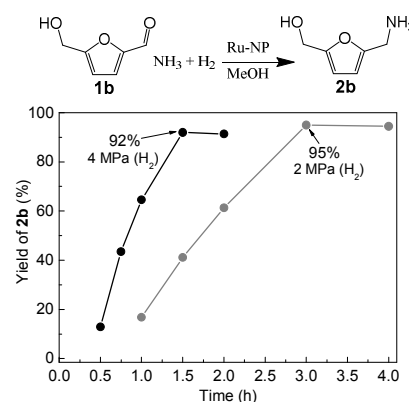

Fig. 5 Time courses of reductive amination of 5-hydroxymethylfurfural (**1b**) over Ru-NP. Reaction conditions: Catalyst (0.2 mg), **1b** (0.5 mmol), MeOH (5 mL), NH_3 (8 mmol), and H_2 (2 and 4 MPa), 363 K.
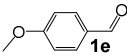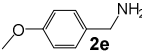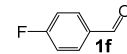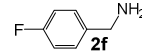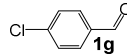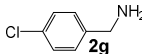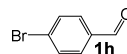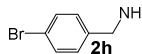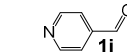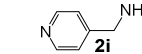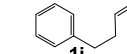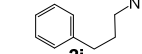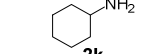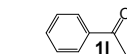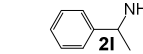
Table 3 Comparison of primary amines production from various aldehydes and ketones over the Ru-NP and Ru/Nb_2O_5 catalysts^a

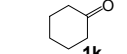| Entry	Substrate	Time (h)	Product	Yield^b (%)		TOF (h^{-1})		R_{Ru-NP}^{c}
				Ru-NP	Ru/Nb_2O_5	Ru-NP	Ru/Nb_2O_5	
1	**1b**	3	**2b**	95	39	730	140	5.2
2	**1c**	2	**2c**	68	29	780	150	5.2
3	**1d**	4	**2d**	95	34	550	90	6.1

Please do not adjust margins

Chemical Science

Page 6 of 8

View Article Online
DOI: 10.1039/C8SC01197D

Journal Name

ARTICLE

4	1e (4-methoxybenzaldehyde)	4	2e	92	35	530	90	5.9
5	1f (4-fluorobenzaldehyde)	2	2f	94	30	1080	160	6.7
6	1g (4-chlorobenzaldehyde)	2	2g	90	28	1030	150	6.9
7	1h (4-bromobenzaldehyde)	2	2h	93	33	1070	170	6.3
8	1i (pyridine-carbaldehyde)	2	2i	88	31	1010	160	6.3
9	1j (3-phenylpropanal)	2	2j	97	35	1110	180	6.2
10	1k (cyclohexanone)	1	2k	97	43	2230	450	5.0
11	1l (acetophenone)	3	2l	98	38	750	130	5.8

[a] Reaction conditions: catalyst (0.2 mg for Ru-NPs; 20 mg for 1 wt% Ru/Nb$_2$O$_5$), substrate (0.5 mmol), MeOH (5 mL), NH$_3$ (8 mmol), H$_2$ (2 MPa), 363 K. [b] GC yield. [c] R_{Ru-NP} defined the ratio of TOFs for Ru-NP and Ru/Nb$_2$O$_5$.

In comparison with the efficient supported metal catalyst Ru/Nb$_2$O$_5$ (Table 3), Ru-NP showed prominently higher TOFs and operated with a reaction rate approximately 5~7 times higher for production of various primary amines by reductive amination of these carbonyl compounds.

Conclusions

In summary, flat-shaped pristine fcc Ru NPs, consist of high atomically active {111} facets on the flat surfaces were constructed as a high performance catalyst. The specific flat-shaped morphology and surface electronic structure of Ru NPs clearly contributes to their outstanding catalytic performance, as reflected by exceptionally high TOFs observed for the reductive amination of several carbonyl compounds, compared to the conventional efficient supported metal catalysts. The Ru-NP catalyst also exhibits excellent durability and selectivity during prolonged recycling. Shape-specific Ru NPs are available as a benchmark catalyst for the efficient production of various primary amines, particularly the important biomass-based amine intermediates. The present Ru-NP catalyst is also expected to be widely applicable for the metal-catalyzed production of several indispensable chemical resources, which is still a challenge for the chemical industry with conventional supported metal catalysts.

Conflicts of interest

There are no conflicts to declare.

Acknowledgements

Notes and references

1 L. He, F. Weniger, H. Neumann and M. Beller, *Angew. Chem. Int. Ed.*, 2016, **55**, 12582-12594.
2 B. C. Gates, *Chem. Rev.*, 1995, **95**, 511-522.
3 A. M. Ruppert, K. Weinberg and R. Palkovits, *Angew. Chem. Int. Ed.*, 2012, **51**, 2564-2601.
4 P. Munnik, P. E. de Jongh and K. P. de Jong, *Chem. Rev.*, 2015, **115**, 6687-6718.
5 M. Hara, M. Kitano and H. Hosono, *ACS Catal.*, 2017, **7**, 2313-2324.
6 S. Crossley, J. Faria, M. Shen and D. E. Resasco, *Science*, 2010, **327**, 68-72.
7 N. Zheng and G. D. Stucky, *J. Am. Chem. Soc.*, 2006, **128**, 14278-14280.
8 C. Xiao, T.-W. Goh, Z. Qi, S. Goes, K. Brashler, C. Perez and W. Huang, *ACS Catal.*, 2016, **6**, 593-599.
9 R. Fang, H. Liu, R. Luque and Y. Li, *Green Chem.*, 2015, **17**, 4183-4188.
10 P. Pachfule, X. Yang, Q.-L. Zhu, N. Tsumori, T. Uchida and Q. Xu, *J. Mater. Chem. A*, 2017, **5**, 4835-4841.
11 M. Kitano, Y. Inoue, Y. Yamazaki, F. Hayashi, S. Kanbara, S. Matsuishi, T. Yokoyama, S.-W. Kim, M. Hara and H. Hosono, *Nat. Chem.*, 2012, **4**, 934-940.
12 C. T. Campbell, *Acc. Chem. Res.*, 2013, **46**, 1712-1719.
13 C. T. Campbell and J. R. V. Sellers, *Chem. Rev.*, 2013, **113**, 4106-4135.
14 R. Schlögl, *Angew. Chem. Int. Ed.*, 2015, **54**, 3465-3520.
15 K. An and G. A. Somorjai, *ChemCatChem*, 2012, **4**, 1512-1524.
16 A. T. Bell, *Science*, 2003, **299**, 1688-1691.
17 G. Ertl, *Angew. Chem. Int. Ed.*, 2008, **47**, 3524-3535.
18 J. Ohyama, T. Sato, Y. Yamamoto, S. Arai and A. Satsuma, *J. Am. Chem. Soc.*, 2013, **135**, 8016-8021.
19 A.-X. Yin, W.-C. Liu, J. Ke, W. Zhu, J. Gu, Y.-W. Zhang and C.-H. Yan, *J. Am. Chem. Soc.*, 2012, **134**, 20479-20489.

Chemical Science Accepted Manuscript

Chemical Science Accepted Manuscript

20 S. H. Joo, J. Y. Park, J. R. Renzas, D. R. Butcher, W. Huang and G. A. Somorjai, *Nano Lett.*, 2010, **10**, 2709-2713.
21 K. Kusada, H. Kobayashi, T. Yamamoto, S. Matsumura, N. Sumi, K. Sato, K. Nagaoka, Y. Kubota and H. Kitagawa, *J. Am. Chem. Soc.*, 2013, **135**, 5493-5496.
22 Y. Inoue, M. Kitano, K. Kishida, H. Abe, Y. Niwa, M. Sasase, Y. Fujita, H. Ishikawa, T. Yokoyama, M. Hara and H. Hosono, *ACS Catal.*, 2016, **6**, 7577-7584.
23 A. M. Karim, V. Prasad, G. Mpourmpakis, W. W. Lonergan, A. I. Frenkel, J. G. Chen and D. G. Vlachos, *J. Am. Chem. Soc.*, 2009, **131**, 12230-12239.
24 W.-Z. Li, J.-X. Liu, J. Gu, W. Zhou, S.-Y. Yao, R. Si, Y. Guo, H.-Y. Su, C.-H. Yan, W.-X. Li, Y.-W. Zhang and D. Ma, *J. Am. Chem. Soc.*, 2017, **139**, 2267-2276.
25 J. Kang, S. Zhang, Q. Zhang and Y. Wang, *Angew. Chem. Int. Ed.*, 2009, **48**, 2565-2568.
26 A. Chen, T. Miyao, K. Higashiyama, H. Yamashita and M. Watanabe, *Angew. Chem. Int. Ed.*, 2010, **49**, 9895-9898.
27 T. Abe, M. Tanizawa, K. Watanabe and A. Taguchi, *Energy Environ. Sci.*, 2009, **2**, 315-321.
28 K. S. Hayes, *Appl. Catal. A*, 2001, **221**, 187-195.
29 S. Imm, S. Bähn, L. Neubert, H. Neumann and M. Beller, *Angew. Chem. Int. Ed.*, 2010, **49**, 8126-8129.
30 B. Chen, U. Dingerdissen, J. G. E. Krauter, H. G. J. Lansink Rotgerink, K. Möbus, D. J. Ostgard, P. Panster, T. H. Riermeier, S. Seebald, T. Tacke and H. Trauthwein, *Appl. Catal. A*, 2005, **280**, 17-46.
31 M. Pera-Titus and F. Shi, *ChemSusChem*, 2014, **7**, 720-722.
32 I. Delidovich, P. J. C. Hausoul, L. Deng, R. Pfützenreuter, M. Rose and R. Palkovits, *Chem. Rev.*, 2016, **116**, 1540-1599.
33 P. Roose, K. Eller, E. Henkes, R. Rossbacher and H. Höke, in *Ullmann's Encyclopedia of Industrial Chemistry*, Wiley-VCH Verlag GmbH & Co. KGaA, **2015**, DOI: 10.1002/14356007.a02_001.pub2, pp. 1-55.
34 J. L. Klinkenberg and J. F. Hartwig, *Angew. Chem. Int. Ed.*, 2011, **50**, 86-95.
35 J. Kim, H. J. Kim and S. Chang, *Eur. J. Org. Chem.*, 2013, **2013**, 3201-3213.
36 A. K. Holzer, K. Hiebler, F. G. Mutti, R. C. Simon, L. Lauterbach, O. Lenz and W. Kroutil, *Org. Lett.*, 2015, **17**, 2431-2433.
37 T. Gross, A. M. Seayad, M. Ahmad and M. Beller, *Org. Lett.*, 2002, **4**, 2055-2058.
38 J. Gallardo-Donaire, M. Ernst, O. Trapp and T. Schaub, *Adv. Synth. Catal.*, 2016, **358**, 358-363.
39 C. F. Winans, *J. Am. Chem. Soc.*, 1939, **61**, 3564-3565.
40 C. Schäfer, B. Nişanci, M. P. Bere, A. Daştan and B. Török, *Synthesis*, 2016, **48**, 3127-3133.
41 K. V. R. Chary, K. K. Seela, D. Naresh and P. Ramakanth, *Catal. Commun.*, 2008, **9**, 75-81.
42 Annemieke W. Heinen, Joop A. Peters and Herman v. Bekkum, *Eur. J. Org. Chem.*, 2000, **2000**, 2501-2506.
43 S. Gomez, J. A. Peters, J. C. van der Waal, W. Zhou and T. Maschmeyer, *Catal. Lett.*, 2002, **84**, 1-5.
44 J. Bódis, L. Lefferts, T. E. Müller, R. Pestman and J. A. Lercher, *Catal. Lett.*, 2005, **104**, 23-28.
45 B. Dong, X. Guo, B. Zhang, X. Chen, J. Guan, Y. Qi, S. Han and X. Mu, *Catalysts*, 2015, **5**, 2258.
46 S. Nishimura, K. Mizuhori and K. Ebitani, *Res. Chem. Intermed.*, 2016, **42**, 19-30.
47 T. Komanoya, T. Kinemura, Y. Kita, K. Kamata and M. Hara, *J. Am. Chem. Soc.*, 2017, **139**, 11493-11499.
48 M. Chatterjee, T. Ishizaka and H. Kawanami, *Green Chem.*, 2016, **18**, 487-496.
49 Y. Nakamura, K. Kon, A. S. Touchy, K.-i. Shimizu and W. Ueda, *ChemCatChem*, 2015, **7**, 921-924.
50 S. R. Kirumakki, M. Papadaki, K. V. R. Chary and N. Nagaraju, *J. Mol. Catal. A*, 2010, **321**, 15-21.
51 When CO was adsorbed on Ru-NP (20), a band was observed at 2027 cm^{-1} with a shoulder (ca. 2035 cm^{-1}) assignable to CO adsorbed on flat-shaped fcc Ru NPs (Figure S8). These results suggest that flat-shaped Ru NPs are mixed with large hcp Ru NPs in Ru-NP (20); Ru-NP (20) has a higher TOF than Ru-HCP (Table 1) although the diffraction peaks due to hcp Ru are mainly observed in the XRD pattern for Ru-NP (20).
52 X. Shao, S. Prada, L. Giordano, G. Pacchioni, N. Nilius and H.-J. Freund, *Angew. Chem. Int. Ed.*, 2011, **50**, 11525-11527.
53 J. Liu, *ChemCatChem*, 2011, **3**, 934-948.
54 E. A. Carbonio, M. J. Prieto, A. d. Siervo and R. Landers, *J. Phys. Chem. C*, 2014, **118**, 28679-28688.
55 K. Qadir, S. H. Joo, B. S. Mun, D. R. Butcher, J. R. Renzas, F. Aksoy, Z. Liu, G. A. Somorjai and J. Y. Park, *Nano Lett.*, 2012, **12**, 5761-5768.
56 K. Qadir, S. M. Kim, H. Seo, B. S. Mun, F. A. Akgul, Z. Liu and J. Y. Park, *J. Phys. Chem. C*, 2013, **117**, 13108-13113.
57 A. Corma, S. Iborra and A. Velty, *Chem. Rev.*, 2007, **107**, 2411-2502.
58 M. Hara, K. Nakajima and K. Kamata, *Sci. Technol. Adv. Mater.*, 2015, **16**, 034903.
59 The kinetic parameters were estimated by fitting the time course of the concentration of 3a and 2a on the assumption that the reaction is sequential. The attempts to reproduce the reaction profile was unsuccessful likely because the present reductive amination cannot be simply explained by the sequential reaction and the reaction mechanism is complicated as mentioned in our previous paper. The detailed reaction mechanism and kinetic parameters including the reaction order and activation energy of each step are currently under investigation.
60 T. Ayusawa, S. Mori, T. Aoki, R. Hamana, US Patent 4598159, 1986.
61 E. Bayram, J. C. Linehan, J. L. Fulton, J. A. S. Roberts, N. K. Szymczak, T. D. Smurthwaite, S. Özkar, M. Balasubramanian and R. G. Finke, *J. Am. Chem. Soc.*, 2011, **133**, 18889-18902.
62 E. Bayram and R. G. Finke, *ACS Catal.*, 2012, **2**, 1967-1975.
63 S. Kanbara, M. Kitano, Y. Inoue, T. Yokoyama, M. Hara and H. Hosono, *J. Am. Chem. Soc.*, 2015, **137**, 14517-14524.
64 T.-N. Ye, J. Li, M. Kitano, M. Sasase and H. Hosono, *Chem. Sci.*, 2016, **7**, 5969-5975.
65 M. Kitano, S. Kanbara, Y. Inoue, N. Kuganathan, P. V. Sushko, T. Yokoyama, M. Hara and H. Hosono, *Nat. Commun.*, 2015, **6**, 6731.
66 S. Y. Chin, C. T. Williams and M. D. Amiridis, *J. Phys. Chem. B*, 2006, **110**, 871-882.
67 E. Guglielminotti, F. Boccuzzi, M. Manzoli, F. Pinna and M. Scarpa, *J. Catal.*, 2000, **192**, 149-157.
68 K. Nakajima, R. Noma, M. Kitano and M. Hara, *J. Phys. Chem. C*, 2013, **117**, 16028-16033.
69 Y. Yancai, H. D. Sheng, L. Yue, F. Xiaoqian, W. Xin, Y. Peiqun, H. Xun, Z. Gang, W. Yuen and L. Yadong, *Angew. Chem.*, 2016, **128**, 5591-5595.
70 B. Liu and Z. Zhang, *ChemSusChem*, 2016, **9**, 2015-2036.

Table of content entry

Chemical Science Accepted Manuscript